ELSEVIER

Chemical Geology 228 (2006) 175–196

CHEMICAL GEOLOGY
INCLUDING
ISOTOPE GEOSCIENCE

www.elsevier.com/locate/chemgeo

The nexus between groundwater modeling, pit lake chemogenesis and ecological risk from arsenic in the Getchell Main Pit, Nevada, U.S.A.

Andy Davis [a,*], T. Bellehumeur [a], P. Hunter [a], B. Hanna [a], G.G. Fennemore [b], C. Moomaw [a], S. Schoen [b]

[a] *Geomega, 2995 Baseline Road, Suite 202, Boulder, CO 80303, United States*
[b] *Barrick Gold Corporation, Crescent Valley, NV 89821, United States*

Accepted 6 November 2005

Abstract

The proliferation of mine pits that intersect the groundwater table has engendered interest in the environmental consequences of the lakes that form after cessation of dewatering. The Getchell Main Pit (GMP) in Nevada hosts arsenic sulfide (As_xS_y) mineralization (e.g., orpiment and realgar) and ambient groundwater As up to 1.8 mg L^{-1}, making groundwater inflow a potentially significant As source to the future pit lake. Predictive simulations using MODFLOW-SURFACT show that the GMP lake water level will recover to within 99% of the pseudo-equilibrium stage within 100 years after the end of dewatering, resulting in a 75-m deep, terminal pit lake. The juvenile GMP lake (after 5 years) will be a calcium sulfate, pH 7.8 water body containing 920 mg L^{-1} TDS and 0.6 mg L^{-1} As evolving towards a pH 7.9, 1580 mg L^{-1} TDS and 0.9 mg L^{-1} As water body after 100 years. The predicted pit lake chemistry is consistent with earlier pit lake water quality after 16 years when the South and Center Pits, precursors to the Main Pit, were allowed to fill during a mining hiatus (1968–1984). The GMP mature pit lake chemistry was used to assess ecological risk to potential local receptors, i.e., mallard duck, cliff swallow, golden eagle, little brown bat, spotted sandpiper, deer mouse, mule deer and cattle. Arsenic does not strongly bioaccumulate through the food chain at Getchell; hence, pit lake As will not pose an unacceptable risk.

Keywords: Arsenic; PITQUAL; Ecological risk; Getchell Mine; Pit lake

1. Introduction

Cessation of dewatering activities at open pit mines results in the creation of a "pit lake" if the pre-mining groundwater table elevation is higher than the bottom of the pit after it is decommissioned. As part of the environmental assessment process, it is necessary to determine the potential environmental impacts of the future pit lake chemistry on (1) groundwater quality adjacent to the pit and (2) probable ecological receptors.

Existing pit lakes pre-date the onset of pit lake chemistry predictions, while those for which predictions have been made are yet to fill, hence, model verification has proved difficult. There have been several papers describing the chemistry of existing pit lakes (e.g., Davis and Ashenburg, 1989; Eary, 1999; Shevenell et al., 1999; Parshley and Bowell, 2003). However, with

* Corresponding author. Tel.: +1 303 938 8115; fax: +1 938 8123.
E-mail address: andy@geomega.com (A. Davis).

0009-2541/$ - see front matter © 2006 Elsevier B.V. All rights reserved.
doi:10.1016/j.chemgeo.2005.11.023

the exception of a bench-scale test (Davis, 2003) and an analysis of the North Pit lake at Getchell (Tempel et al., 2000), there appears to be a paucity of literature pertaining to "prediction" of pit lake chemistry and its implications on post-mining uses, especially considering their number worldwide, and in particular in the western United States. For example, in Nevada alone, there are projected to be at least 35 such features that either currently contain water or will upon termination of mining at the facilities (Shevenell et al., 1999).

This paper describes a pit lake water quality study undertaken at the Getchell Main Pit (GMP), Humboldt County, ~90 km north of Golconda, NV (Fig. 1). Of particular interest in this setting is the elevated naturally occurring background arsenic (As) found in the local soils (270 mg kg^{-1}) and groundwater (1.8 mg L^{-1}) in the area.

Computing the future pit lake water quality (Fig. 2) requires initial water quantity modeling, in this case using MODFLOW-SURFACT (HydroGeoLogic, 1996), to determine the rate of infilling of the pit lake and the flow proportions through each lithologic unit (Geomega, 2003a). These data were used as inputs to PITQUAL (Davis et al., 2001), which accounts for the solute leachability from each wall rock lithology, and in combination with the flow velocity, computes temporal mass loading into the pit. The resulting bulk chemistry was input to PHREEQC (Parkhurst, 1995) to determine the dissolved pit lake chemistry, allowing chemogenetic trends to be developed (Geomega, 2003b). Finally, the predicted mature pit lake chemistry was used to assess the potential for ecological risk (Geomega, 2003c) based on a deterministic dose model (EPA, 1993a,b).

For the Main Pit lake predictions, calibration of the groundwater flow model was based on a 35-year record of environmental data. The geochemical model calibration was compared to empirical laboratory test results (leaching, geotechnical, geochemical, etc.). Uncertainty in groundwater and geochemical model results were quantified with statistical tests and with sensitivity analyses, where critical parameters (e.g., recharge) were varied by ±10%. Additionally, both models were

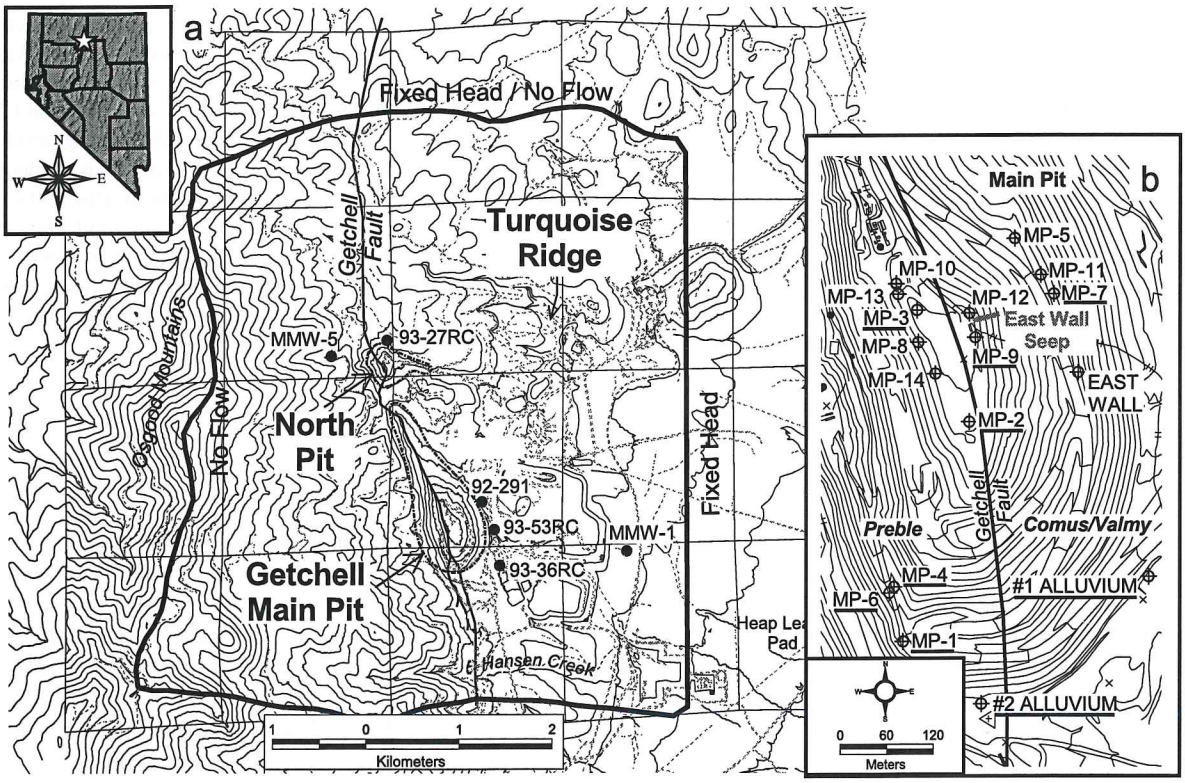

Fig. 1. (a) Getchell model domain with 30 m topographic contours showing the location of the GMP, North Pit and Turquoise Ridge underground mine, the model boundary conditions and a subset of the monitoring wells used in transient calibration of the model (Fig. 6); and (b) GMP lithologies, showing locations for the seep samples (data in Table 2), and the GMP UPS samples with the subset used in humidity cells (Table 1) underlined. Topographic contours are 6 m.

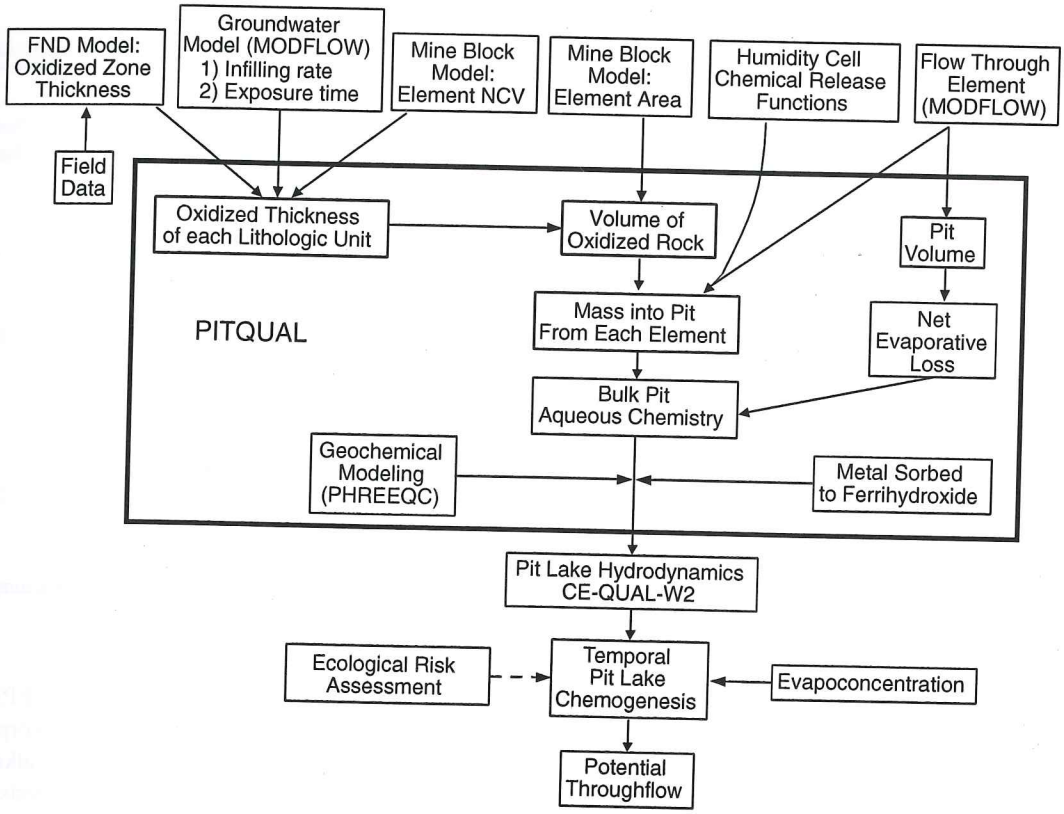

Fig. 2. Elements of pit lake chemogenetic modeling showing data and model integration.

verified by comparison of pit water quantity and quality predictions to data from the two transitory pit lakes that formed in the Center and South Pits from 1968 to 1984.

The ecological risk assessment (ERA) incorporated biological data collected at Getchell to develop soil/plant uptake and bioaccumulation factors through the food web. By applying uncertainty factors in measures of effects, the ERA adhered to the tenets of the Precautionary Principle based on U.S. EPA algorithms (U.S. EPA, 1998) by ensuring that these measures were sufficiently protective of assessment endpoints.

1.1. Mining and dewatering history

Elevations range from 2225 m above mean sea level (m amsl) at the peak of the Osgood Mountains west of the mine to 1525 m amsl at the Getchell Mine heap leach pad. The metamorphic and sedimentary Osgood Mountains trend north–south (Fig. 1) and have been extensively thrust faulted and intruded by a granodiorite stock.

The GMP is an amalgamation of the historical South and Center Pits, which were originally excavated from the late 1930s through 1968. When mining operations were discontinued in 1968, the attendant pit lakes recovered by 1984 to a near-equilibrium stage. By 1982, the Center Pit was ~40 m deep with a ponded surface area of 3.2×10^4 m^2, while the South Pit was ~25 m deep with a ponded surface area of 5.3×10^4 m^2. When mining operations resumed in 1984, water was pumped from the pit lakes (1984–1987), while from 1987 to 1992 dewatering operations for further pit excavation consisted of pumping from sumps in the base of the pit (Fig. 3). Between 1992 and 1995, perimeter wells were installed to dewater the adjacent bedrock. By this time, the two historical pits had been deepened and merged to form the ~130 m deep, 8.5×10^5 m^2 GMP.

The North Pit, independent of the Center and South Pits, was also excavated and had the same filling/dewatering history, although it was shallower (34 m) than the future Main Pit lake (76 m) will be. In the future, the North Pit will remain dry, even when the Main Pit reaches a steady-state stage because of runoff diversions around the North Pit, increased evaporative losses and dewatering operations in adjacent mining areas. The historical North Pit lake was the subject of a

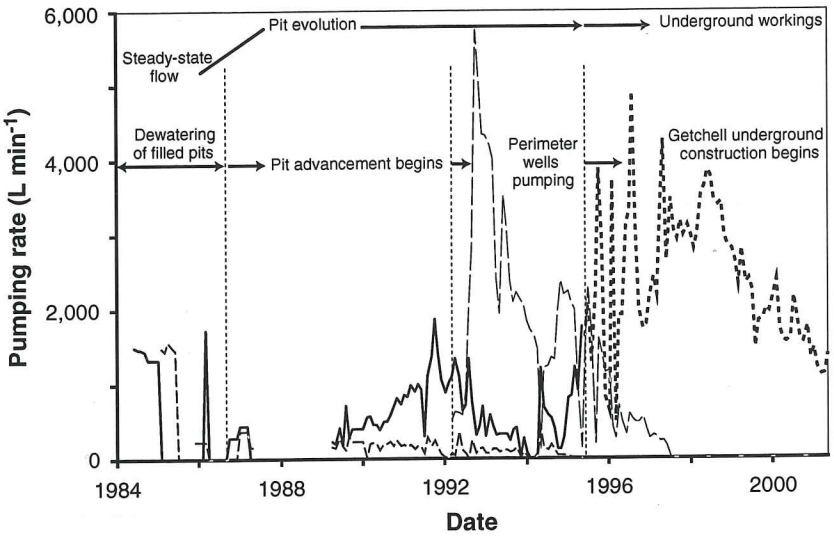

Fig. 3. Historic dewatering at Getchell. The different pumping eras represent dewatering of the Center Pit sump (——), the South Pit sump (– –), total pit perimeter pumping (—) and the underground sump in the Main Pit (- - -).

prior modeling exercise (Tempel et al., 2000), which simulated the pit lake chemistry over an 8.5-year period when the pit was at close to steady state conditions.

Beginning in 1994, the Getchell Underground Mine was developed from the base (1500-m elevation) of the GMP via three adits in the western pit wall. Mining continues with ~42 km of underground workings extending beneath the pit to the 1400-m elevation. Presently, the underground workings are dewatered by a system of sumps that are pumped to a booster station located at the bottom of the GMP. Underground dewatering operations maintain dry workings and, in doing so, also keep the GMP dewatered.

1.2. Analytical methods

Humidity cell leachate was collected using the methods of Sobek et al. (1978) and immediately filtered through a 0.45-μm cellulose acetate high capacity filter, preserved (using HNO_3 for metals, H_2SO_4 for nitrogen, and 4 °C for cations and anions) and shipped overnight under chain of custody for analysis.

For groundwater and leachate, temperature, pH, Eh and specific conductance were measured on sample collection using an Orion 290A for pH, a Hach Sension1 for Eh and a Fisher Scientific digital conductivity meter for specific conductance (with all equipment calibrated daily). Major anions were analyzed using ion chromatography (EPA 300.0), major cations by inductively coupled plasma (ICP) optical emission spectroscopy (OES) following EPA method 200.7, dissolved metals using ICP mass spectrometry (MS) by EPA method 200.8, dissolved mercury using atomic absorption (AA) cold vapor using EPA method 245.1, and alkalinity, pH and total dissolved solids (TDS) by methods SM 2320 B, SM 4500 H+B and SM2450 C, respectively (U.S. EPA, 1993a,b). Analytical quality assurance and quality control (QA/QC) measures met EPA (1988) criteria.

1.3. UPS geology and chemistry

The Getchell deposit is hosted by the Cambrian Preble, Ordovician Comus and Ordovician Valmy formations (Groff et al., 1997). The Preble Formation units west of the Getchell fault are gray-colored marble and silicified skarn, with some black carbonaceous hornfels (Roswell et al., 1979). The granodiorite intrusives are exposed in the pit wall as veins within the Preble Formation, or as a yellowish unit in the upper elevations in the northern end of the GMP, while the black and tan Valmy and Comus Formation volcanic units outcrop in the eastern highwalls of the GMP (Fig. 1).

One hundred and eleven samples representative of each UPS rock type were collected from the GMP and tested for paste pH and specific conductivity. A subset of 36 of these was analyzed for sulfate sulfur, sulfide sulfur, carbonate, acid base accounting (ABA) and bulk metals (Table 1). The net neutralization potential (NNP) ranged from −122 to +808 and pH from 4.4 to 9.0, demonstrating that both acid-neutralizing and potentially acid-generating rock is exposed in the pit walls.

Table 1
Whole rock chemistry and acid–base accounting

Sample	Lithology	$\%S^{6+}$	$\%S^{2-}$	AGP[a]	ANP[a]	NNP[a]	pH[b]	As	Fe
#1 alluvium[c]		<0.01	<0.01	<0.3	11	11	7.9	680	22,000
#2 alluvium[c]		<0.01	<0.01	<0.3	10	10	7.8	670	22,000
NHC-6	Carbonaceous	0.05	0.05	1.6	18	16	7.5	43	9000
NHC-7	Carbonaceous	0.01	0.04	1.3	12	11	8.1	19	6900
HC-6	Carbonaceous	0.05	0.29	9.1	8.3	−0.8	4.4	240	9800
HC-4	Carbonaceous	0.21	0.68	21	7.1	−14	5.7	410	18,000
NP-6	Carbonaceous hornfels	0.13	1.07	33	12	−21	5.9	2200	11,000
MP-1	Granodiorite[c]	0.02	0.12	3.8	27	24	8.3	200	22,000
GU 4775-1	Granodiorite	0.20	2.1	66	12	−54	4.7	1500	24,000
GU 4700	Granodiorite	0.18	0.18	5.6	89	83	8.7	87	27,000
NP-1	Granodiorite	<0.01	<0.01	<0.3	14	14	8.0	63	24,000
MP-2	Hornfels[c]	0.30	0.24	7.5	68	60	7.6	180	38,000
NP-7	Hornfels[c]	0.28	0.24	7.5	419	412	6.9	12,000	14,000
MP-4	Hornfels[c]	0.10	0.9	28	530	502	8.3	3000	12,000
GW 4775-2	Hornfels	0.48	0.41	13	310	297	9.2	49	21,000
MP-3	Marble[c]	0.17	0.45	14	498	484	8.1	76	9600
MP-6	Marble[c]	0.10	0.25	7.8	706	698	9.0	2100	8300
NP-2	Marble	0.24	4.96	160	38	−122	6.5	76,000	14,000
NHC-1	Marble	<0.01	<0.01	<0.3	16	16	8.3	290	31,000
HC-8	Marble	<0.01	<0.01	<0.3	5.9	5.9	7.8	22	8400
GU 4665	Marble	0.38	0.41	13	674	661	7.7	300	14,000
GU 4850	Marble	0.04	0.02	0.6	43	42	8.1	20	26,000
GU 4850d	Marble	0.15	0.01	0.3	63	62	7.9	89	26,000
NHC-8	Marble	<0.01	<0.01	<0.3	808	808	8.0	47	5000
HC-2	Marble	0.31	1.09	34	767	733	8.1	130	14,000
NP-5	Sediment	0.08	0.24	7.5	29	21	7.7	250	36,000
NHC-4	Shear zone	1.2	7.3	230	757	527	7.6	340	65,000
HC-5	Silicified	<0.01	<0.01	<0.3	4.1	4.1	7.5	1200	24,000
NP-8	Tuff	0.40	2.3	72	26	−46	4.8	48	64,000
MP-7	Volcanics	0.19	0.65	20	27	7	8.7	24	53,000
MP-9	Volcanics[c]	0.54	0.41	13	61	48	7.0	79	34,000
NP-4	Volcanics	0.30	1.5	47	18	−29	7.6	160	38,000
TR-2	Volcanics	<0.01	<0.01	<0.3	24	24	9.0	23	35,000
TR-5	Volcanics	0.09	0.06	1.9	1.4	−0.5	6.6	230	20,000
TR-6	Volcanics	0.32	0.24	7.5	270	263	7.6	2600	25,000
TR-10	Volcanics	0.06	0.18	5.6	3.5	−2.1	7.4	160	33,000
Typical NV soils[d]		–	–	–	–	–	–	0.1–100	0.01→10

AGP=acid generating, ANP=acid neutralizing and NNP=net neutralizing potential.
All concentrations in mg kg^{-1} unless otherwise noted.
[a] ppt $CaCO_3$.
[b] Paste pH in standard units.
[c] Located in Fig. 1.
[d] From Shacklette and Boerngen (1984).

Sulfide sulfur was detected in 80% of the whole rock samples, indicating that positive NNPs are due to excess carbonate content rather than a lack of sulfide sulfur. Despite the presence of sulfides, paste pH tests showed that 87% of the rock materials were acid-neutralizing.

A preponderance (80%) of Preble Formation units contain <1% sulfide, with isolated pockets in the hornfels up to 7.3% (Table 1). The marble and skarn units are exclusively acid-neutralizing, while ~50% of the hornfels are potentially acid-generating. Enriched metal concentrations correspond to the presence of sulfides ($p=0.99$) and are associated with local mineralization (Table 1).

Approximately half of the granodiorite units are potentially acid-generating with As associated with the mineralized zone (Table 1). The Valmy and Comus units contain low but detectable sulfide (<0.01–2.4%; Table 1). Net neutralization potential (NNP) range from −46 to 263, with four of eight samples potentially acid generating. Average bulk As (the element of most

environmental concern) in all mineralized pit wall materials (Table 1) are above typical Nevada soils (Shacklette and Boerngen, 1984).

The Getchell Mine orebody and country rock contains abundant orpiment (As_2S_3), realgar (AsS), arsenopyrite (FeAsS) and arsenian pyrite (FeS_2 enriched in As) in the sulfide zone (Groff et al., 1997), which result in elevated metal concentrations when in equilibrium with groundwater (Grimes et al., 1995), i.e.,

$$AsS + 3.5H_2O + 2.25O_{2(aq)} = 3H^+ + As(OH)_4^- + SO_4^{2-} \quad (1)$$

$$As_2S_3 + 8H_2O + 6O_{2(aq)} = 8H^+ + 2As(OH)_4^- + 3SO_4^{2-} \quad (2)$$

$$FeAsS + 2.5H_2O + 2.75O_{2(aq)} = H^+ + As(OH)_4^- + SO_4^{2-} + Fe^{++} \quad (3)$$

$$FeS_2 + H_2O + 3.5O_{2(aq)} = 2H^+ + 2SO_4^{2-} + Fe^{++} \quad (4)$$

Although pyrite reaction rates are up to 15 times faster than realgar and orpiment under acidic (pH 2) conditions (Lengke, 2001), the arsenic sulfides oxidize more rapidly than pyrite at circum-neutral pH (7–8) explaining the naturally elevated As in mineralized site groundwater (Table 2).

1.4. Site groundwater chemistry

The water chemistry from two seeps that flow at <3.8 L min^{-1} from the volcanic units in the eastern wall and granodiorite in the north wall of the Main Pit represent the future chemistry of groundwater and runoff inflows from these units. These waters generally meet drinking water standards (Table 2) except for As (0.16 mg L^{-1} versus a standard of 0.05 mg L^{-1}), which is toward the low end of the range of baseline groundwater As. The granodiorite unit seep is typical of neutralized leachate (Table 2), e.g., pH 7.6, As=0.004 mg L^{-1}, SO_4=2000 mg L^{-1} and TDS=3200 mg L^{-1}.

The naturally elevated deep groundwater metal condition is illustrated by water chemistry in boreholes in the adjacent Turquoise Ridge underground mine (Fig. 1) where artesian water flowing from three boreholes drilled to 215–335 m in Area 148 (~1175 m amsl) was sampled from a depth well below any anthropogenically induced oxidation reactions. The groundwater chemistry from artesian bores TU00-699, TU00-700 and TU00-849 (Table 2) is circum-neutral, containing naturally

Table 2
Site groundwater chemistry

Lithology	Drinking water standard[a]	TU00-699	TU00-849	TU00-700	East wall seep[b]	North end seep	Sump
		Fault zone Preble	Fault zone Preble	Fault zone Preble	Comus/Valmy	Granodiorite	Preble
pH[c]	6.5–8.5	7.65	7.55	7.63	7.44	7.56	8.09
TDS	500 (1000)	460	430	460	690	3200	420
Alkalinity		110	100	100	270	7	78
NO_3	10	<0.05	<0.05	<0.05	<0.05	<0.5	<0.05
Ca		80	76	94	130	550	82
Mg	150 (180)	19	20	20	38	150	7.6
K		3.8	3.4	3.8	5	12	2.6
Na		36	38	32	34	83	20
Cl	400	44	41	43	31	100	26
F	2 (4)	0.35	0.34	0.27	<0.1	1	0.25
SO_4	250 (500)	190	180	200	230	2000	190
Al	0.1	<0.05	<0.05	<0.05	<0.05	2.7	<0.05
As	0.05	1.8	1.5	0.36	0.16	0.004	0.93
Ba	2	0.056	0.072	0.042	0.068	0.018	0.022
B		0.08	0.09	0.12	0.14	0.11	0.12
Cu	1	<0.002	<0.002	<0.002	0.002	0.071	0.002
Fe	0.3 (0.6)	<0.05	<0.05	<0.05	<0.05	<0.05	<0.05
Mn	0.05 (0.1)	0.044	0.04	0.04	0.07	12	0.014
Ni	0.1	0.002	0.002	0.004	0.004	0.11	0.006
Zn	5	<0.02	<0.02	<0.02	<0.01	0.72	<0.01

Concentrations in mg L^{-1} unless otherwise noted.
[a] Nevada primary and (secondary) drinking water standards.
[b] Location marked on Fig. 1.
[c] Standard units.

Table 3
Summary of baseline groundwater chemistry in the vicinity of Getchell Mine

	Getchell Mine Site						USGS Basin Wide (Grimes et al., 1995)					
	N^a	BDL[b]	%BDL	Min	Max	Mean	N	BDL	%BDL	Min	Max	Mean
pH[c]	436			6.1	9	7.6	471	0		6.5	8.8	7.8
NO_3	307	80	26	<0.1	5.5	1.5	450	296	66	<0.1	460	2.2
Ca	303	0	0	18	234	105	487	0	0	10	380	65
Mg	303	0	0	3.1	65	22	486	0	0	2	96	21
K	303	1	0	1.2	9.1	3.8	486	0	0	2.2	6200	26
Na	318	0	0	22	137	44	487	0	0	5	190	46
Cl	318	0	0	8.1	504	86	477	0	0	7.7	7200	65
SO_4	427	0	0	18	550	195	479	0	0	4	640	116
Sb	208	173	83	<0.001	0.069	0.002	488	75	15	<0.0001	2.4	0.02
Al	172	123	72	<0.05	1.5	0.1	488	485	99	<0.1	<1	0.06
As	358	74	21	<0.001	7.7	0.13	488	59	12	<0.001	2.6	0.04
Ba	271	4	1	0.008	0.22	0.06	144	0	0	0.005	0.25	0.05
Cd	303	296	98	<0.03	0.03	0.001	421	254	60	0.00002	0.025	0.001
Cr	271	166	61	<0.05	0.05	0.008	486	336	69	<0.00009	0.0067	0.0004
Ag	271	251	93	<0.0005	0.036	0.001	421	413	98	<0.000008	0.0004	0.0001
Cu	303	175	58	<0.001	0.19	0.01	488	215	44	<0.001	0.03	0.003
Fe	272	72	26	<0.02	21	0.88	488	284	58	<0.01	48	0.15
Pb	271	226	83	<0.001	0.031	0.002	485	441	91	<0.00003	0.024	0.001
Mn	276	125	45	<0.001	4.4	0.27	632	57	9	0.001	1.6	0.179
Hg	318	310	97	<0.0005	0.004	3E−04	0					
Ni	208	38	18	<0.002	0.085	0.02	488	82	17	0.001	0.6	0.014
Tl	208	206	99	<0.02	0.02	0.001	144	126	88	<0.0002	0.004	0.001
Zn	303	229	76	<0.01	0.5	0.02	488	51	10	<0.0004	1.2	0.021

Concentrations in mg L^{-1} unless otherwise noted.
[a] Number of analyses.
[b] Below method detection limit.
[c] Standard units.

occurring As (up to 1.8 mg L^{-1}). Sump water quality, reflecting accumulated drainage into the underground workings is similar to the deep groundwater quality (Table 2). Influent baseline groundwater quality used in PITQUAL was based on summary statistics from the Getchell Mine seeps, sump and area monitoring well network, along with the USGS (Grimes et al., 1995) local area database (Tables 2 and 3).

2. Water quantity modeling

MODFLOW-SURFACT (HydroGeoLogic, 1996), an enhanced version of the three-dimensional finite-difference groundwater flow code MODFLOW (McDonald and Harbaugh, 1988), was used to simulate groundwater flow. The basic MODFLOW-SURFACT flow module was employed, supported by the block-centered flow 4 (BCF4, with variable saturation option), evapotranspiration (EVT), recharge-seepage face boundary (RSF4), well (WEL1), horizontal flow barrier (HFB), drain (DRN), lake (LAK2), interbed storage (IBS), adaptive time stepping and output control (ATO4), and the preconditioned conjugate gradient 4 solver (PCG4). The automated calibration tool WinPEST (Doherty, 1998) was used to optimize model parameters during calibration.

2.1. Discretization of model domain

The model domain (3×10^7 m^2) includes the section of the Kelly Creek Basin extending from the western edge of the basin at the peak of the Osgood Mountains to ~5 km east of that flow divide (Fig. 1). The north, south and western edges of the model domain are approximate groundwater flow divides, with groundwater generally flowing from west to east, from the Osgood Mountains to Kelly Creek. The orientation of the grid is such that the horizontal axis follows the general direction of groundwater flow to provide the highest resolution, both laterally and vertically in the pit area and at the pit perimeter pumping wells. In plan view, the model domain was divided into 49 columns and 61 rows, in which the dimensions of the smallest cell is 60 m × 30 m × 30 m and the largest is 210 m × 210 m × 520 m (Fig. 4a).

The model domain was divided into 13 horizontal layers to simulate the vertical range, extending from an elevation of 640 m amsl to the ground surface (Fig. 4b).

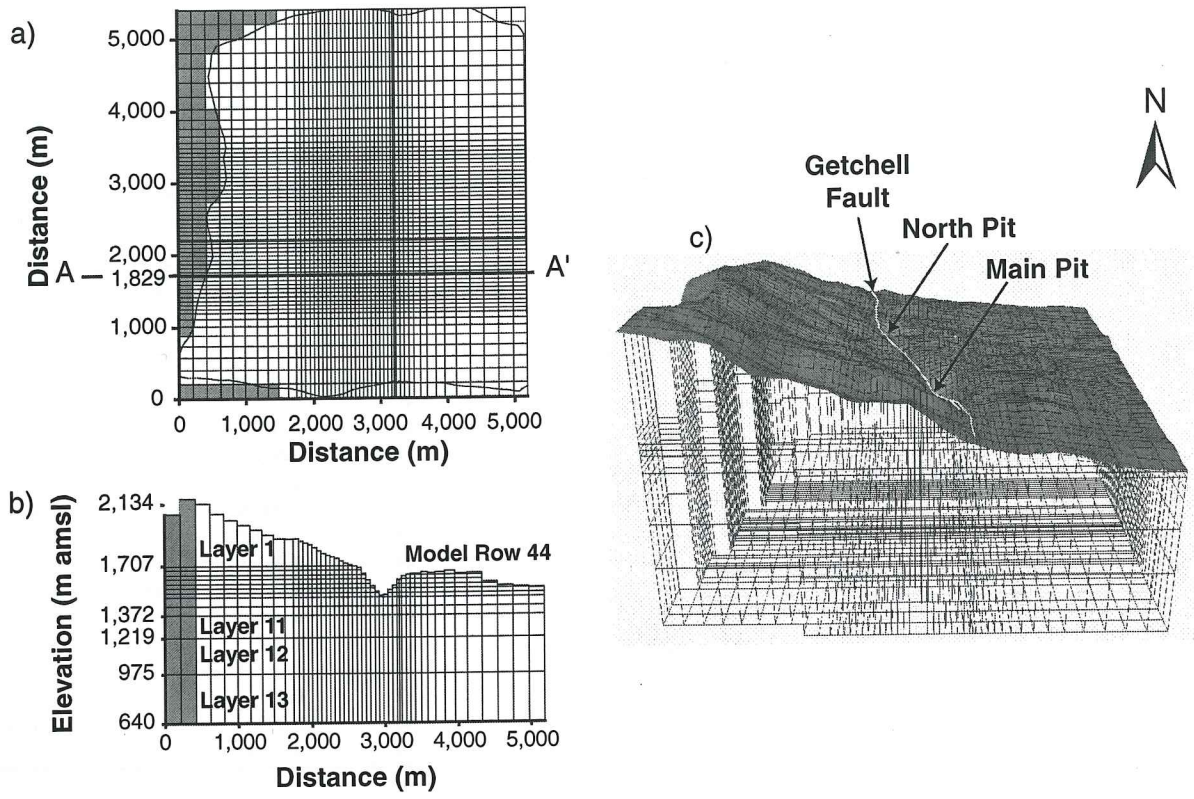

Fig. 4. Getchell model grid showing size and relative cell density: (a) plan view, (b) cross section (through section A–A′ identified on a) and (c) 3-D grid.

The thickness of the model (915–1525 m) allows for potential deep flow through bedrock. Topographic information was obtained from a digital contour map (3–6 m contour intervals) from the Getchell Mine to develop a digital elevation map (Fig. 4c).

2.2. Subsurface features

The Getchell Fault (Fig. 1) displays a right-lateral strike-slip movement off-setting all formations (Hobbs, 1948) with a sufficiently shallow dip (55°NE) that a vertical structure in the model would not adequately represent the hydraulic behavior near the pit areas. Therefore, the fault was represented as a unique lithologic unit of low conductivity projected into the subsurface to ensure three-dimensional connectivity of fault cells and eliminate the possibility of groundwater flow bypassing the fault.

Consistent with Anderson and Woessner (1992) and Larocque et al. (1999), underground workings were represented by assigning equivalent porous medium (EPM) properties to ~200 model cells intersecting underground workings (elevation range from 1620 to 1370 m amsl).

Storage parameter values for the EPM cells were calculated by adding the primary porosity of the country rock (2.8%) and the void space corresponding to underground workings in each model cell (0.6–10%). Sump pumping was simulated in the model by using the drain (DRN) package for MODFLOW. Model recharge was applied to the highest active cell within each vertical column using the recharge package (RSF4) in MODFLOW-SURFACT. The average annual net evaporation rate specified for the lake surface during recovery was 0.81 m $year^{-1}$, calculated as the difference between adjusted pan evaporation (1.17 m $year^{-1}$) based on historical data from Rye Patch Dam in the Humboldt River basin and Ruby Lake in northeastern Nevada (Shevenell, 1996), and precipitation (0.36 m $year^{-1}$).

2.3. Model calibration, uncertainty and results

The root mean square error (RMSE) of a calibrated steady-state model should be <10% of the range of observations (Spitz and Moreno, 1996). For the Getchell model, the normalized RMSE was 1.6% based on a model RMSE of 6.7 m compared to a 430-m range of observed water levels. The mean error of the calibrated

model was −0.9 ft, indicating that the model is not biased towards overestimating or underestimating the measured water levels. The cumulative sump flow and dewatering rates for 1985–1995 (compare slopes in Fig. 5a) are also closely matched.

The transient model from 1996 to 2001 was calibrated by varying the hydraulic conductivities of the underground working EPM cells. For this period, the predicted cumulative flow to the underground sumps was within 97% of the dewatered volume of water from the underground workings (Fig. 5b), while the predicted sump flow rate at the end of 2001 (1430 L min^{-1}) compares favorably to the measured sump flow rate (1390 L min^{-1}) at that time in the underground workings. Model-predicted and measured water levels for the transient case are also well matched at both ends of the GMP (Fig. 6). On aggregate, model calibration exceeded EPA (1992) and ASTM (1996) criteria.

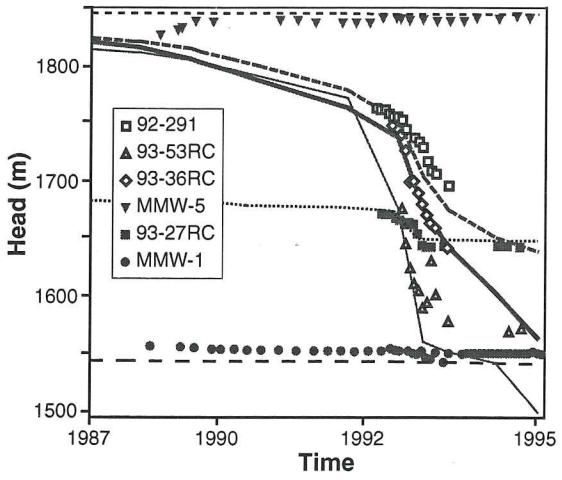

Fig. 6. Comparison of simulated vs. observed water levels (transient calibration) for wells outside (93-27RC, MMW-1, MMW-5), south of (93-36RC) and around (92-291, 93-22RC, 93-53RC) the GMP area. Well locations shown on Fig. 1.

2.4. Predictive simulations

Water-level recovery began in the lowest lake cell elevation in the GMP (1504 m amsl) at time zero (Fig. 7), representing the end of mining in 2013. After 10 years of recovery, the lake stage is predicted to be 1530 m amsl. Fifty years after the cessation of mining, the lake water level will recover 85% and, after 100 years, it will recover to within 99% of the pre-mining condition when the lake stage reaches an equilibrium level of 1580 m amsl, with the deepest part at 76 m. The computed volume of the lake 100 years after mining is 6.8×10^6 m^3 with a surface area of 2×10^5 m^2.

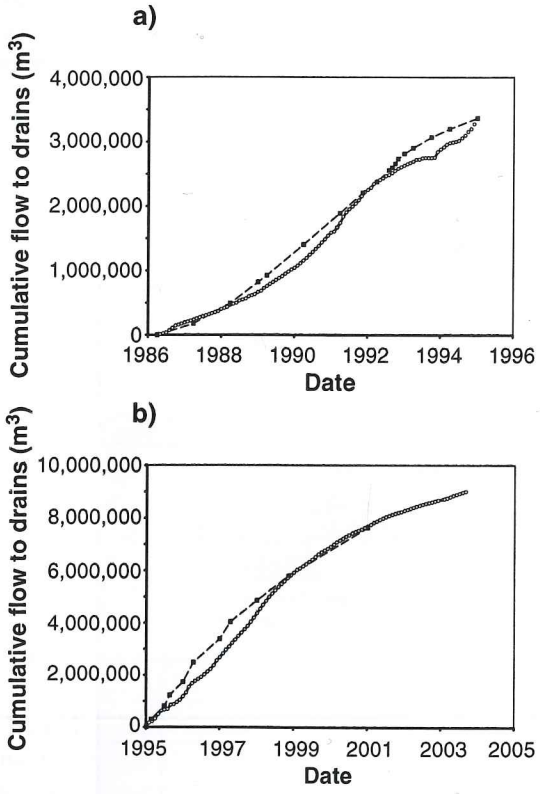

Fig. 5. Predicted (OO) and measured (■) flow to sumps during (a) 1987–1995 and (b) 1995–2002.

Inflows from the underground workings, via three adits in the west wall of the GMP, account for ~29% of the pit inflow during early lake refilling (<5 years) increasing to ~33% over the 100-year refilling period (Fig. 8). The remainder of the pit inflows come primarily from the higher-permeability Comus/Valmy volcanics in the eastern pit wall during the first 25 years of refilling, and then from higher elevation Preble Formation and Comus/Valmy volcanics as the pit lake stage recovers to elevations >1550 m. Relative inflows from the granodiorite in the northern end of the pit lake are small (4–8%) compared to the volume of inflow through other units, but are significant to future pit lake chemistry because of their poor leachate quality.

The GMP lake surface elevation will be about 60 m lower than the Center and South Pits water level in 1982 because of the increased lake surface and, therefore, increased evaporation. Upon refilling, groundwater flow will be directed toward the pit lake because evaporation from the lake surface causes it to act as a groundwater sink. Hence, the Main Pit lake will be a terminal water body with no through-flow component.

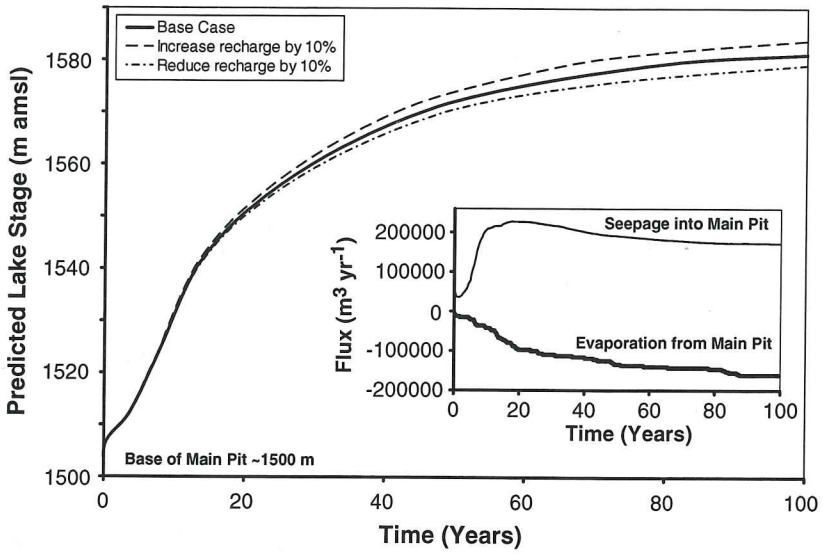

Fig. 7. Simulated GMP lake stage recovery. The base case was tested for uncertainty assuming that infiltration varied by ±10%. Inset shows seepage and evaporation.

2.5. Uncertainty in the groundwater model

The sensitivity of the groundwater model to parameter variability was assessed by varying boundary condition assumptions and changing input variables to cover a reasonable range of expected conditions.

2.5.1. Sensitivity from eastern model boundary

A combination of dewatering operations at the Getchell Mine and/or at the nearby Twin Creeks Mine have lowered the water levels on the eastern boundary of the Getchell model domain, such that a decreasing hydraulic head of 1.2 m year^{-1} was assigned to these

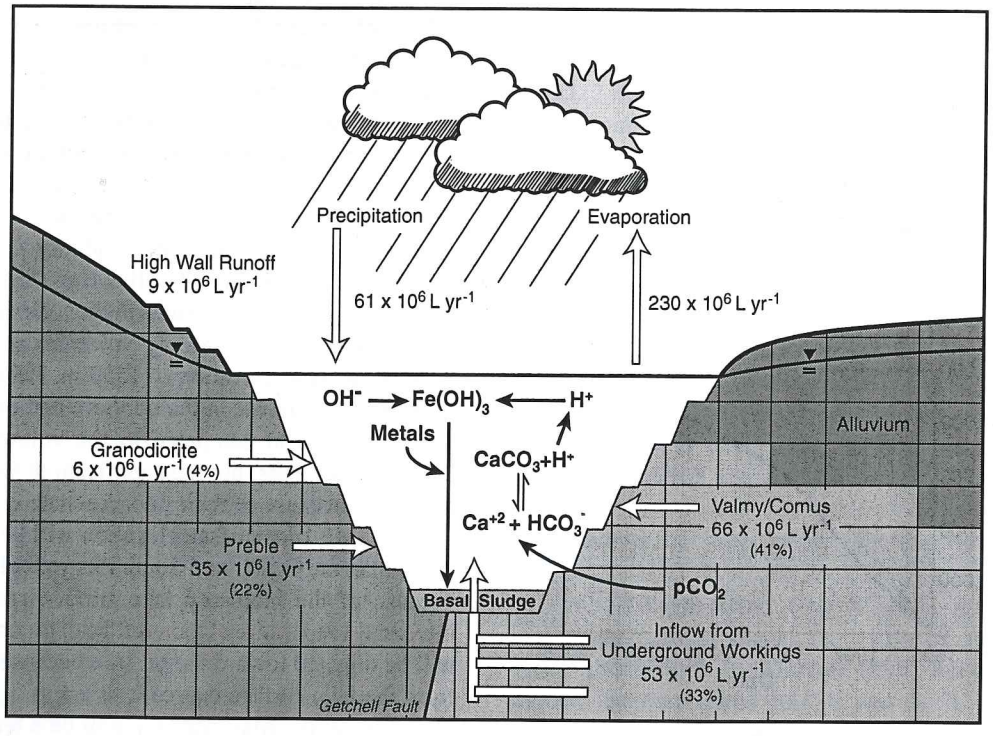

Fig. 8. Schematic of geochemical process controlling the ultimate pit lake chemistry and various elements of the mature GMP lake water budget.

fixed head boundaries in the base case simulation. Four different scenarios of the eastern model boundary fixed heads were evaluated: (1) no drawdown of the eastern model boundary; (2) more rapid decrease in the fixed head boundary of 2.3 m $year^{-1}$ for 10 years of continued mining and 10 years after mining ends; (3) decrease in the fixed head boundary for a longer period (10 years longer than the base case); and (4) decrease fixed boundary heads for a shorter period (1.2 m $year^{-1}$ for 10 years of continued mining). The predicted ultimate lake stage, for different fixed water levels on the eastern model boundary, ranged from 1576 to 1586 m amsl demonstrating that the predicted lake infilling rates and stage are relatively insensitive (±5 m) to the foreseeable head distribution on the eastern model boundary.

2.5.2. *Sensitivity from recharge*

The impact of greater or lower recharge at the Getchell Mine over the next century was evaluated in the predictive pit filling simulation by increasing and decreasing model recharge over the entire model domain by 10% compared to that estimated using the Berger (2000) method. The predicted ultimate Main Pit lake stage for the increased recharge scenario was 3 m higher and was only 2 m lower for lower model recharge, demonstrating the relative insensitivity of the model to this parameter.

3. Pit lake chemogenesis

Predicting the pit lake chemogenetic pathway (Fig. 2) requires input of (1) ultimate pit surface (UPS) wall rock leachability (typically from humidity cells), (2) contribution from the underground workings (from sump and borehole aqueous chemistry), (3) the oxidized zone thickness in the UPS, (4) the flow and leachate chemistry from each UPS lithology, (5) geochemical speciation of the bulk fluid at each time period and (6) evapoconcentration over the time frame of the prediction. Additionally, the proclivity for pit lake turnover was assessed using CE-QUAL-W2 (Cole and Wells, 2002) to assess effects of potential stratification, particularly with respect to the stability of precipitated amorphous ferric hydroxide (AFH).

3.1. *Wall rock leachate chemistry*

Humidity cells (Sobek et al., 1978) were used to simulate potential acid generation and determine leachate chemistry as a function of time in the UPS. Humidity cells are a conservative simulation of wall rock leachability because while moist air is employed in the oxidation step for 50% of the time, in practice rock in the humidity cells rarely dries out completely during the dry cycle. Furthermore, the humidity cells only incorporate the <2 mm fraction, whereas in reality a large range of particle sizes are present in the UPS.

Seventeen humidity cell tests were run on rock samples selected to match the overall distribution of NNPs observed in the pit and to represent each of the rock types present in the GMP (i.e., Preble Formation marbles, skarns and hornfels, Valmy/Comus volcanics, and granodiorite, along with smaller exposures of alluvium and intrusive dykes). Leachates were analyzed as described in Section 1.2.

The lowest leachate pH in the 17 cells was 2.7, typically ranging from 3.7 to 8.7 (Fig. 9a), consistent with the range of acid-generating and acid-neutralizing NNP values. The acid-generating material was primarily associated with a small section of granodiorite and Preble Formation hornfels exposed in the north end of the Main Pit, leaching As (up to 28 mg L^{-1}; Fig. 9b), SO_4 (up to 2950 mg L^{-1}) and Fe (up to 5300 mg L^{-1}). Conversely, neutral to alkaline leachate contained SO_4<200 mg L^{-1}, and As and Fe at their method detection limits (0.002 mg L^{-1} and 0.05 mg L^{-1},

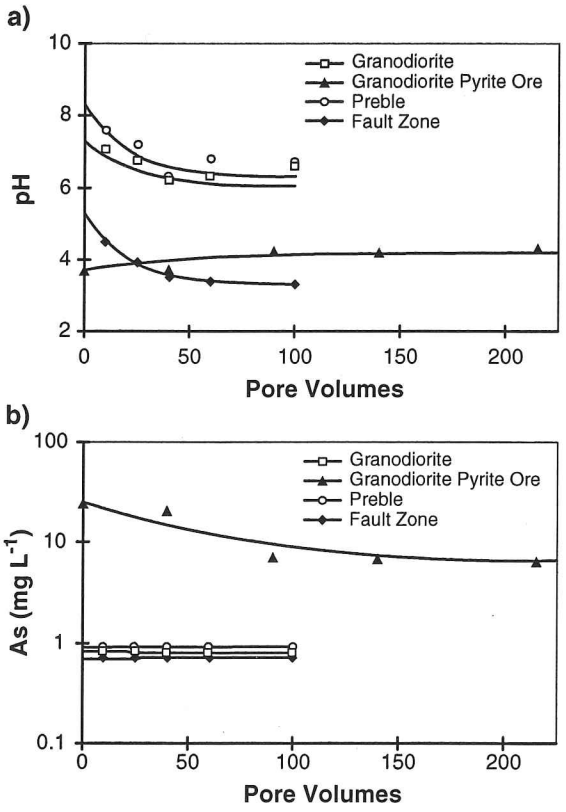

Fig. 9. Typical humidity cell effluent chemistry for (a) pH and (b) As.

respectively). The charge balances on leachate tests were generally less than ±10% with an average absolute imbalance of 8%, indicating that analyses were sufficiently complete and accurate.

3.2. Chemical release functions (CRFs)

CRFs were fit to the humidity cell data using either a constant, exponential, exponential squared or an inverse function to determine the bulk leachate chemistry input to PITQUAL (Fig. 2). The background groundwater chemistry associated with each lithology in the pit surface was used to set the asymptotic limit of the CRFs to ensure that the water quality emanating from thoroughly leached wall rock would be consistent with the background groundwater chemistry and not underestimated.

3.3. Sulfide oxidation rates

As the excavation advances, the air-filled porosity of the rock in the immediate vicinity of the pit increases because of dewatering and creation of additional fractures by blasting. With increasing distance into the rock from the UPS, the air-filled porosity decreases as the effects of blasting are muted. Therefore, sulfides oxidize most readily in a veneer of UPS wall rock where atmospheric oxygen is available via fracture and porosity-controlled air movement into the pit wall.

Sulfide oxidation was modeled using the Fennemore–Neller–Davis (FND) modification of the Davis–Ritchie approach (Fennemore et al., 1999) to simulate wall rock reactivity in arid climates. The dominant sulfides consume different amounts of oxygen during oxidation, i.e., pyrite 1.7 g O_2 g^{-1} S, orpiment 2.3 g O_2 g^{-1} S and realgar 2.7 g O_2 g^{-1} S. Assuming that each mineral oxidizes completely and congruently over the period of interest, the total O_2 consumption was normalized to the relative sulfide compositions (50% orpiment, 25% realgar and 25% pyrite) resulting in an aggregate 2.2 g O_2 g^{-1} S. The diffusion rate of oxygen through the rock material was determined from calibration of the model to measured humidity cell effluent sulfate concentrations (Fig. 10). The rate of sulfide oxidation in the field has been determined to be four times slower than that observed in humidity cells (Fennemore et al., 1999). However, since site-specific field oxidation rates were not available, the accelerated rates observed in humidity cells were used to preclude underestimation of As leaching.

Subsequently, the FND model output was used to determine UPS oxidized thicknesses for each block in the geochemical model on an annual basis [assigned as Preble Formation marble and skarn (30%), granodiorite (25%) and Valmy/Comus Formation volcanics (45%)] assuming that oxidation will cease after inundation. This is a reasonable assumption because diffusion of oxygen in air is three orders of magnitude higher than diffusion of oxygen in water (Davis and Ritchie, 1986), greatly reducing the oxidation rates following inundation of sulfide.

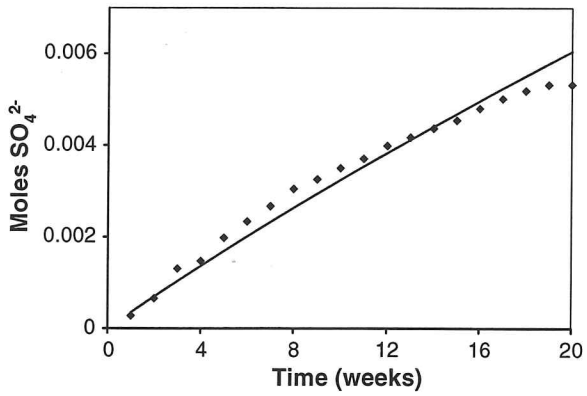

Fig. 10. Sulfide oxidation model calibration to the Valmy/Comus humidity cell data.

3.4. Bulk pit lake chemistry

The precipitation, evaporation and net evaporation volumes were calculated on an annual basis using the MODFLOW Lake Package as the pit fills and the surface area of the pit lake increases (Fig. 8). The volume of net evaporation, calculated from the product of the net evaporation rate and the surface area of the pit lake, increased over time because the pit surface area increases during refilling until a pseudo-equilibrium condition is attained.

The volume of surface water runoff from the pit walls was determined by calculating the surface area of each rock type above the water level in the UPS using the ArcInfo Triangulated Irregular Network (TIN) module. As the pit refills over 100 years, runoff from outside the pit area will be diverted by the storm water diversion in place around the pit. However, because the walls and benches will ultimately slope to the bottom of the pit, all precipitation falling on the UPS wall rock area was assumed to run off into the pit. The volume of runoff was calculated from the product of the wall rock area and an average annual precipitation of 0.35 m $year^{-1}$. The volume of wall rock runoff decreases as the pit refills, inundating previously exposed wall rock and reducing the total exposed wall rock surface area. In

general (Fig. 8), the volume of wall rock runoff is small (1×10^7 L year^{-1}) compared to the volumes of evaporation (23×10^7 L year^{-1}) and groundwater inflow (16×10^7 L year^{-1}).

The bulk chemistry inputs to the juvenile pit lake are dominated by the wall rock leachate until ~25 years, after which contributions from the background groundwater predominate. The bulk chemistry of the volume of water entering through each rock unit was determined by integrating the CRF for each model cell with respect to pore volume over the period of interest and, summing the integrals by rock type, resulting in an aggregate bulk chemistry for each analyte at that time.

In PITQUAL, influent waters were proportionally mixed with the existing volume of antecedent pit water from the previous year to derive the net volume of water in the pit based on the pit-filling model. PITQUAL mixes the relative proportions of i water sources (V_i) to arrive at the total water volume (V_{tot}) in the pit, i.e.,

$$V_{tot} = \sum_{i=1}^{n} V_i$$

where n is the number of water sources. The mixing ratio M_i is defined as:

$$M_i = \frac{V_i}{V_{tot}}$$

These computations identify the proportion of water derived from each wall rock unit filling the GMP (Fig. 8) and the percentage from the antecedent pit lake.

3.5. Dissolved pit lake chemistry

Within the PITQUAL shell, PHREEQC (Parkhurst, 1995) was run in cumulative 1-year incremental time steps over 100 years to determine the final annual dissolved pit lake water quality. At each time increment, the pathway incorporated hydrogeochemical constraints (Fig. 8), including (1) proportional mixing of influent and antecedent waters, (2) evapoconcentration of the mixed pit lake water, (3) equilibration of the solution with atmospheric and groundwater gases (e.g., O_2, CO_2), (4) solution equilibration with potential solid phases [e.g., amorphous ferric hydroxide (AFH)], (5) computation of the solid mass precipitated from solution, (6) sorption of solutes to AFH, (7) speciation and equilibration of the resulting pit solution and (8) input of the solution to the next year's simulation. At each modeling step, influent and antecedent waters (including the pit lake solution) were charge balanced with sulfate to maintain electrical neutrality.

The calculated P_{CO_2} of the historical pit lakes was $10^{-2.96}$, slightly higher than the atmospheric value ($10^{-3.5}$), but consistent with the hypothesis that lake CO_2 levels should be elevated above atmospheric levels (Cole et al., 1994). Solid phases predicted to be oversaturated in the historical pit lake water columns (Fig. 8) included calcite (SI=+1.0) and AFH (SI=+1.9). Thus, the P_{CO_2} was set at 10^{-3} and the potential precipitation of calcite and AFH was accommodated in PITQUAL.

3.6. Adsorption to amorphous ferric hydroxide

Field data and laboratory experiments have shown that AFH is the first Fe phase to precipitate from solution as Fe^{2+} is oxidized (Langmuir and Whittemore, 1971; Schwertmann and Taylor, 1977). The precipitation of AFH sequesters both cations and anions from solution by coprecipitation and adsorption (Fig. 8) as a function of pit lake pH (Davis and Eary, 1997; Kalin et al., 2000).

In PITQUAL, sorption was modeled by computing the mass of AFH precipitated on an annual basis, then using the double layer model (DLM) with the appropriate intrinsic stability constants (Dzombak and Morel, 1990) to calculate the distribution of an element between dissolved and surface (adsorbed) forms. While the specific surface area of AFH has been reported to range between 160 and 720 m^2 g^{-1} (Davis and Leckie, 1978; Dzombak and Morel, 1990), the specific surface area (220 m^2 g^{-1}) measured for precipitate formed in the analogous Gold Quarry sorption study (PTI, 1992) was used for the Getchell study. The mass of AFH precipitated in prior years was not allowed to contribute sorptive surface area, based on the assumption that the floc will settle to the base of the pit each year.

3.7. Evapoconcentration

The water quality of lakes in arid regions of the western U.S. can be affected by evaporative water loss and subsequent solute evapoconcentration (Miller et al., 1996). The volume of water lost to evaporation from the GMP was determined from the product of the annual net evaporation rate (1.17 m year^{-1}) and the surface area of the pit lake, after the water inflow in the current time increment had been added to the lake. Total lake surface area as a function of increasing water level was determined by planimetry of the UPS topography. Using the evaporated portion of the entire pit lake volume, PHREEQC calculated the appropriate fraction of pit water to be removed via calculation of the evaporation ratio. Solute concentrations, activities and

saturation indices in the remaining water mass were then re-calculated at each time step. The geochemical code was also verified against the evapoconcentration study of Garrels and MacKenzie (1967).

In general, evaporation increases solute concentrations and facilitates precipitation of solids. The volume reduction is represented by the evapoconcentration factor (μ), which in the GMP will be 2.3 over the 100-year model period, primarily controlled by the surface area to depth ratio (76 m deep: 2.0×10^5 m^2).

3.8. Model results

The pH of the pit lake will increase from 7.6 to 7.9 over the first 22 years as wall rock leachate mixes with alkaline influent water, after which the pH will remain stable through year 100 (Fig. 11a). This result is due to increasing carbonate concentrations during evaporation, while P_{CO_2} remains constant and equilibrium with calcite is maintained. The pit lake is also projected to have moderate alkalinity (Fig. 11b).

Adsorption to AFH in the GMP lake will control As. The annual AFH production ranges from a maximum of 17.5 mg L^{-1} in year 1 to a minimum of 0.4 mg L^{-1} by year 100, corresponding to an AFH production of 637 kg in the first year and to 2740 kg by year 100. This result is consistent with the findings of Kalin et al. (2000) who observed reductions in the Fe mass precipitated over the initial years of pit lake formation in Saskatchewan. Arsenic in the mature pit lake is predicted to be 0.93 mg L^{-1} (Fig. 11c), above the drinking water standard (0.05 mg L^{-1}), but within the range reported for the baseline groundwater in the vicinity of the Getchell Mine (0.13 to 1.8 mg L^{-1}). The effects of evapoconcentration are apparent in the monotonic increase in As and SO_4 (Fig. 11d). The latter (970 mg L^{-1} in the mature pit lake) acts as a conservative tracer due to its negligible sorption and lack of effective solid phase solubility constraints in this system.

3.9. Model validation

A lengthy analytical record is available from the historical Center and South Pit lakes (precursors to the Main Pit) that filled between 1968 and 1984 when mining underwent a hiatus at Getchell. These water bodies were initially acidic (pH 3–4) with high Fe (5–32 mg L^{-1}) and SO_4 (~3500 mg L^{-1}) and low As (<0.1 mg L^{-1}). However, these conditions were ephemeral (Fig. 12) with SO_4 decreasing to ~1400 mg L^{-1} as the influent groundwater diluted the original flush of SO_4-rich wall rock effluent. Under the initially acidic conditions, jarosite ($KFe_3(SO_4)_2(OH)_6$), identified in dry pits at Getchell and which incorporates up to 2000 mg As kg^{-1} in its structure by substitution of AsO_4^{3-} for SO_4 (Savage et al., 2000), would have been the stable Fe phase.

As the proto-pit lake pH increased to 4 (Fig. 12), jarosite would become unstable, releasing As into solution (Foster et al., 1998). Subsequently, liberated Fe precipitates as AFH causing Fe to decrease to <1 mg L^{-1} and controlling As solubility through sorption

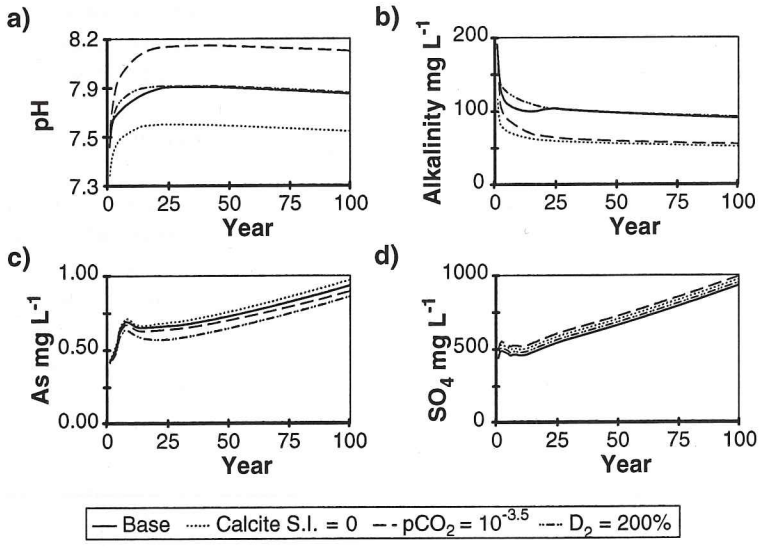

Fig. 11. Predicted pit lake chemogenetic trends for the base case ($pCO_2=10^{-3.0}$ atm., calcite SI=0.5 and $D_2=100\%$) with uncertainty analyses for (a) pH, (b) alkalinity, (c) As and (d) SO_4.

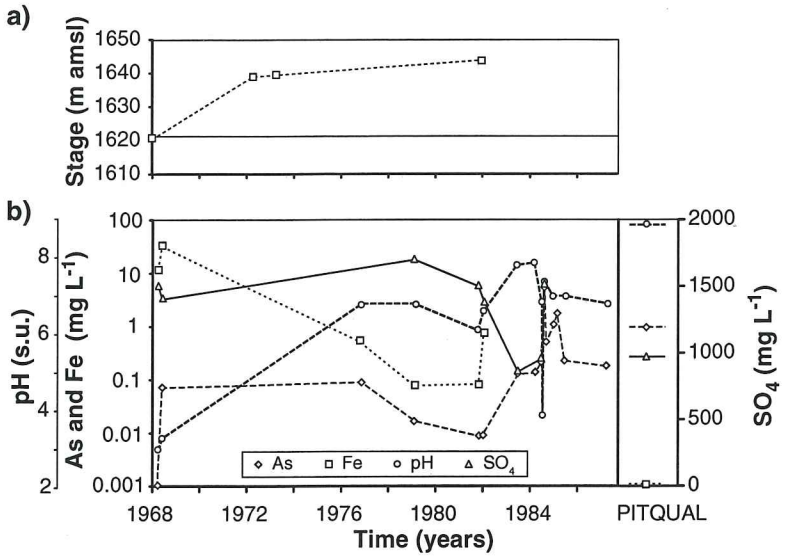

Fig. 12. Historical South Pit lake, (a) stage (1968–1982) and (b) water chemistry (1968–1984) compared to PITQUAL predicted mature GMP lake chemistry.

reactions (Tempel et al., 2000; Kalin et al., 2000). However, As sorption is more effective at mildly acidic conditions than at circum-neutral pH (Drever, 1988), resulting in decreasing Fe with a simultaneous increase in As as the proto-pit lakes transitioned from acidic to neutral pH (Fig. 12).

The final chemogenetic stage in the historical Getchell South and Center Pits comprised pH stabilization near 7 and sulfate ~1000 mg L^{-1}, along with a gradual rise in As to just below 1 mg L^{-1}. During this stage, the contribution of solutes from the UPS diminished, while the background chemistry of the influent water and evapoconcentration of the pit lakes control pit lake chemistry.

While the proto-pit lake chemistry provides valuable insights into future GMP lake trends, the specific chemogenetic trajectory will differ from the historical pit lakes for a number of reasons. Specifically, there will be reduction in the fraction of granodiorite exposed in the GMP wall (Fig. 1), compared to the South and Center Pits, and hence in the relative contribution of seepage through the granodiorite unit (because of its relatively higher location on the GMP wall). The GMP lake will also be deeper than the proto-pit lakes resulting in relatively less evapoconcentration (because of a smaller surface area to depth ratio). The differing geometry will result in an increased volume of the GMP lake, an increased rate of infilling (due to the larger groundwater gradient which will be present in the dewatered pit) and an increase in the ratio of pit lake volume to oxidized wall rock volume.

While the historical data for the Getchell South and Center Pits were not used for model calibration or as input to the geochemical model, the predicted chemistry of the GMP is consistent with that of the final chemogenetic stage in the historical Getchell South and Center Pits, providing insite into the likely GMP chemogenetic trends.

3.10. PITQUAL sensitivity analysis

The model calculations are potentially influenced by various elements of uncertainty, i.e., the accuracy of the conceptual model describing the natural system, the variability in experimentally estimated parameters, analytical accuracy and uncertainty in thermodynamic parameters (Eckberg, 2002). A sensitivity analysis was undertaken to assess the effect of variability in (1) pit lake pE, (2) the oxidized rind thickness, (3) the pit lake P_{CO_2} content, (4) calcite saturation indices and (5) thermodynamic data, on the predicted pit lake chemistry.

Comparison of model results for the sensitivity analysis was based on the relative percent difference (RPD) in final values, i.e.,

$$\mathrm{RPD} = \frac{[R_1 - R_2]}{[R_1 + R_2]/2} \times 100$$

where R_1 is the solute concentration from the model simulation and R_2 is the solute concentration from the sensitivity analysis.

3.10.1. Changes in oxidation potential

The influences of changes in the pit lake pE were investigated by varying the pE from 10 to 13 (from the value of 12 used in the PITQUAL model). The pit lake chemistry was insensitive to these variations in oxidation potential (all RPD < 1%).

3.10.2. Changes in the UPS oxidized rind

The oxidized thickness affects the bulk chemistry entering the lake through the UPS in early years by increasing or decreasing the number of pore volumes of water leaching the rock (potentially affecting the CRFs). The predicted UPS oxidized rind thickness is a function of several parameters, of which O_2 diffusion rates are the most sensitive (Geomega, 2003c), so PITQUAL was run at 200% of the calibrated D_2 values and the results compared with the base case. The RPD was 9% for As (due to the preponderance of As sulfides in the wall rock) and 0% for Fe with changing D_2.

3.10.3. Carbon dioxide partial pressure

Carbon dioxide influences the pH of aqueous systems and hence AFH stability and sorbed metal solubility. Model sensitivity was determined by running PITQUAL at P_{CO_2} of $10^{-3.0\pm0.5}$ atm. to bracket the probable ranges of CO_2 in the pit lake. The highest partial pressure ($10^{-2.5}$ atm.) was hypothesized to occur at the sediment/water interface, reflecting the high P_{CO_2} of inflowing groundwater (Cole et al., 1994), and the lowest partial pressure ($10^{-3.5}$ atm) which may occur where the surficial pit lake water is in contact with the atmosphere. The pH ranged from 7.6 at P_{CO_2} $10^{-2.5}$ to 8.1 at P_{CO_2} $10^{-3.5}$ with an RPD in pH of 6% and for As of 10% over this range.

3.10.4. Calcite Saturation Index (SI)

Calcite supersaturation and its attendant influence on pH in surface waters is a common phenomena due to several factors, e.g., increases in temperature, evaporation and/or a loss of CO_2 to photosynthesis or by exsolution to the atmosphere (Langmuir, 1997). The sensitivity of the model to this parameter was evaluated by running PITQUAL at $SI_{calcite}=0.5\pm0.5$. There were only small changes in pH (RPD ~3%), while Fe changed by only −2% and As by +2%.

3.10.5. Thermodynamic data variability

The error propagated by variability in thermodynamic data on model results is a relatively new field of endeavor (Meinrath et al., 2004), yet one that cannot be ignored when the predictions will be used by risk managers to make decisions pertaining to exposed populations. In this study, the uncertainty related to As species formation constants was first examined by running PITQUAL after replacing the existing As thermodynamic data in the MINTEQ database (Allison et al., 1990) with the compilation critically reviewed by Nordstrom and Archer (2003). These data result in a predicted pit lake As of 0.96 mg L^{-1} compared to 0.93 mg L^{-1} for the base case.

In addition, As was speciated using the LJUNGSKILE code (Ödegaard-Jensen et al., 2004), which applies a Latin Hypercube sampling routine (a derivative of the Monte Carlo method) to develop a statistically based variability to formation constants. For the GMP simulations, the pH will be circum-neutral (7–8) and based on LJUNGSKILE, $HAsO_4^{-2}$ (60–99%) and $H_2AsO_4^-$ (1–40%) will be the predominant As species over the range of pH and formation constants evaluated. Carrying As species distribution variability through PITQUAL demonstrated a range of As (from 0.89 mg L^{-1} to 1.07 mg L^{-1}) in the mature pit lake. Hence, error due to uncertainty in the thermodynamic As data is ~±10% in this case.

3.11. Pit lake hydrodynamics

The fate of chemical constituents in a lake are controlled by seasonal changes in water column hydrodynamics (Wetzel, 1983). As spring progresses, the surface water of lakes absorb heat more rapidly than mixing can redistribute. Summer stratification may lead to reduced dissolved oxygen (DO) concentrations in the hypolimnion. The bottom of the pit lakes are predicted to eventually be covered by basal sludge that will consist of AFH floc precipitated from the water column. It is theoretically possible that, under anoxic conditions, precipitated AFH may dissolve; hence, the importance of the oxygen status of the pit lake. The stability of AFH is relevant to the pit lake water quality prediction because of its importance as a metal-sorbing substrate.

To assess the propensity for re-oxygenation, CE-QUAL-W2 (Cole and Wells, 2002), a two-dimensional (longitudinal and vertical), hydrodynamic and water quality model was used to determine the hydrodynamics of the GMP lake at maturity. The model comprised 12 segments each 69 m long, with 32 layers each 3 m deep. Bathymetric profiles were generated for each segment using ArcView©.

Air and dewpoint temperature, wind speed, wind direction and cloud cover data were obtained from the NOAA National Data Center for Elko (1948–2002), Eureka (1983–2002) and Battle Mountain (1949–1954 and 1973–2002), the nearest available stations at similar

elevation to the project area. Data from the three stations were averaged for each parameter to generate an average meteorologic year, which was repeated in the input files for each of the 7 years simulated.

The results of the simulation show that the GMP water column temperatures will increase from February through August and decrease from September through January. The warmest water column temperatures (~21 °C) occur at the surface in July, followed by complete mixing of the water column and relatively uniform temperatures with depth by December. A slight temperature inversion occurs between January through March, where lower temperatures in the overlying epilimnion resulted in potential ice cover during January and February.

Dissolved oxygen ranged from approximately 7.5–11 mg L^{-1}, typically remaining near saturation (9–10 mg L^{-1}) throughout the pit lake (Fig. 13a). The lowest DO was observed at the surface during the summer months where temperatures were >10 °C, but fall turnover in November to December resulted in a uniform DO distribution at >9 mg L^{-1}. In general, the DO profiles are consistent with similar deep lakes, such as Crater Lake and the Anaconda and Yerington pit lakes, that have reported DO from 7–11.5 mg L^{-1} (McManus et al., 1996; PTI, 1996; Miller et al., 1997).

Oxygen profiles were collected from the historical pit lakes at Getchell in January 1982 (Fig. 13b and c) and, although the pit morphologies, inflows and period after pit formation (approaching hydraulic equilibrium but possibly not fully equilibrated) differ from the GMP lake, these pit lakes also remained oxic throughout their profiles except for a sag at the base of the South Pit lake. These data support the hypothesis that DO in the GMP lake will remain at levels conducive to precipitation and stability of AFH throughout the water column.

4. Ecological risk assessment

An ecological risk assessment (ERA) was undertaken to predict the exposure from As to avian and mammalian receptors in the littoral, riparian and near-shore terrestrial areas of the future GMP lake. Risk was evaluated under mature pit lake conditions, because rapid infilling, erosion and wall sloughing during the early years will prohibit substantial development of biological activity. The ERA used the water quality predictions from PITQUAL, empirical site data (soil–plant uptake and soil–mammal bioaccumulation factors) and studies of analog pit lakes in Nevada and elsewhere (e.g., PTI, 1996; Bitterroot, 1999; Kalin et al., 2001).

The vegetative community at the site is a shrubland type dominated by big sagebrush (*Artemisia tridentata* subsp. *tridentata*). Similar to other Nevada pit lakes (PTI, 1996), the mature pit lake is expected to be oligotrophic because of low nutrient (nitrate and

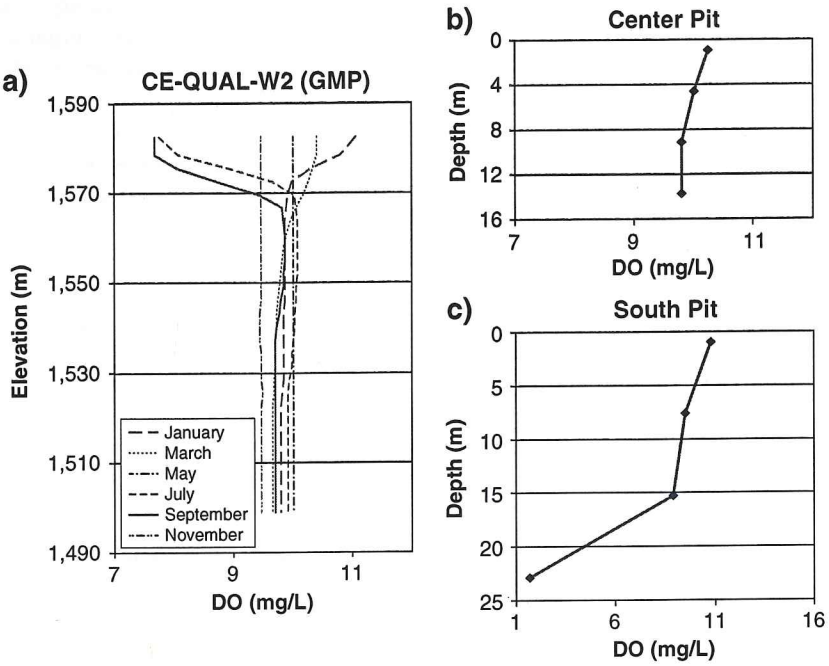

Fig. 13. (a) CE-QUAL-W2 O_2 profile for future GMP and O_2 profiles collected in January 1982 from (b) Center Pit lake and (c) South Pit lake.

phosphate) concentrations and low light penetration owing to the geometry of the pit lake. Eight indicator species were identified, which represent typical exposure of wildlife species to the pit lake, including the mallard duck (*Anas platyrhynchos*), cliff swallow (*Hirundo pyrrhonota*), golden eagle (*Aquila chrysaetos*), little brown bat (*Myotis lucifugus*), spotted sandpiper (*Actitis macularia*), deer mouse (*Peromyscus maniculatus*), mule deer (*Odocoileus hemionus*) and cattle.

4.1. Methods

Exposure was estimated based on a deterministic dose model (EPA, 1993a,b) that integrates site use patterns, food, water, soil or sediment ingestion rates, and other life history characteristics of the receptors, with ingestion the predominant As source to wildlife. The seasonal presence of species was incorporated into the exposure model using an exposure duration term.

Sediment As was estimated from pit wall rock data, aqueous As from the mature GMP lake chemistry and food concentration terms on a receptor-specific basis (Table 4). Foliar As in indigenous plants was measured on aboveground, non-woody biomass from dominant grass and shrub species. Composite samples were collected from seven areas adjacent to the GMP and washed prior to analysis of total As by ICP/MS.

Small mammal As bioaccumulation was computed from mice (*P. maniculatus*) collected in an undisturbed area using Sherman live traps. The mice were sacrificed and stored on dry ice until whole body analysis for As by ICP/MS. Surface soils (upper 15 cm) co-located with plant and mouse collection points were analyzed for As by ICP/MS. Plant and animal data were converted to dry weight to calculate uptake and bioaccumulation factors (UF and BAF, respectively).

Toxicity reference values (TRVs) for comparison to estimated receptor doses were based on phylogenetically similar species exposed via similar routes of exposure (i.e., through diet) with toxicological endpoints comparable to the assessment endpoints. Bioaccumulation of As (and metals in general) can vary widely for aquatic plants and insects depending on species, aqueous geochemistry and other factors (Goodyear and McNeill, 1999; Rainbow, 2002); therefore, only studies conducted under similar field conditions and data for similar plant or invertebrate species likely to be consumed by the ecological receptors was used in the ERA (Table 5).

Table 4
Concentration factors for Getchell trophic levels

Aquatic insectivores	$C_{food} = C_{water} \times BCF_{invert}$	(1)
Terrestrial herbivores	$C_{food} = C_{soil} \times UF_{soil\ to\ plant}$	(2)
Aquatic herbivores	$C_{food} = C_{water} \times BCF_{plant}$	(3)
Tertiary predators	$C_{food} = C_{soil} \times BCF_{soil\ to\ mamm}$	(4)

Table 5
Arsenic bioaccumulation and bioconcentration factors

Factor	Value
BAF soil to mammal[a]	0.04
BCF aquatic invertebrate[b]	8
BCF aquatic plant[c]	15
UF soil to plant[a]	0.09

[a] Site data (Fig. 14).
[b] PTI (1996), Thompson et al. (1972) and U.S. EPA (1985).
[c] Chapman et al. (1998), Chigbo et al. (1982), PTI (1996) and U.S. EPA (1985).

The TRVs were based on No Adverse Effect Levels (NOAELs) and Low Adverse Effect Levels (LOAELs) with uncertainty factors (Ford, 1996; Minteau et al., 1996) applied for interspecies variability. Chronic As toxicity has been relatively well studied in animals, and therefore, TRVs over suitable durations and for suitable non-lethal endpoints (reproduction, development) were available for rodents, ungulates and similar species of passerines compared to indicator species (Table 5). The only chronic studies for mammals and birds were for inorganic forms of As, which are much more toxic at lower doses than organic forms (Vahter and Marafante, 1983; Aposhian, 1997).

However, prey, including invertebrates, birds and mammals, methylate As to organic forms (Rainbow and Dallinger, 1991; Aposhian, 1997; Langdon, 2001), so the TRVs (Table 6) may overestimate risk relative to the As dose to wildlife receptors because much of the As ingested by receptors is probably in the organic form. Risks were characterized by calculating a Hazard

Table 6
Toxicity reference value NOAELs

Receptor	TRV_{NOAEL} Arsenic[a]	TRV_{LOAEL} Arsenic[a]
Cliff swallow[b]	4.1	17.6
Mallard duck[b]	16	71
Golden eagle[b]	2.71	11.8
Spotted sandpiper[b]	4.1	17.6
Little brown bat[c]	1.84	18.40
Mule deer[d]	0.48	0.70
Range cattle[d]	0.36	0.50
Deer mouse[c]	1.27	12.7

[a] mg kg^{-1} day^{-1}.
[b] Stanley et al. (1994).
[c] Schroeder and Mitchener (1971).
[d] James et al. (1966).

Quotient (HQ), the dose/TRV ratio for each receptor. If the HQ_{LOAEL} is >1, risk is likely to exist; for an HQ_{NOAEL} <1 risk is unlikely; while if the HQ_{NOAEL} is >1 and HQ_{LOAEL} is <1, risk is uncertain.

4.2. Results

The site-wide vegetation As uptake factor (mean UF_{plant}=.088) was consistent (Fig. 14) with ORNL (1998). The aggregate As $BAF_{soil/mammal}$ was 0.04 (Table 6), which is higher than that of Sample et al. (1998). However, at Getchell, the entire organism, including the gastrointestinal content (i.e., soil) and adsorbed soil particles on the surface of the animal as well as the body As burden, was analyzed. Bioaccessibility studies of soil and sediment As show that the fraction of absorbed (i.e., bioavailable) As in the gastrointestinal tract of vertebrates is low, typically less than 50% (Davis et al., 1992; Davis et al., 1996; Rodriguez and Basta, 1999).

Arsenic dose concentrations for most receptors were driven primarily by prey ingestion for the receptor species, except for the sandpiper where sediment ingestion was a significant driver. However, because As does not bioaccumulate substantially through the food chain ($BAF_{soil/mammal}$=0.04), dose concentrations did not translate into unacceptable risk. HQ_{NOAEL}'s were <1 for all receptors (Table 7) indicating that adverse effects to these receptors from exposure to As in the surface water, sediments and soils at the GMP lake are unlikely. Indeed, neither the base case pit lake (0.93 mg L^{-1} As) nor the prediction (1.1 mg L^{-1} As based on variable thermodynamic data) would pose an unacceptable risk to avian and mammalian wildlife receptors.

Table 7
Doses (mg kg^{-1} day^{-1}) and hazard quotients for various receptors

Receptor	Dose	HQ_{NOAEL}	HQ_{LOAEL}
Cliff swallow	2.46	0.60	0.14
Deer mouse	0.96	0.76	0.08
Golden eagle	0.14	0.05	0.01
Little brown bat	1.35	0.73	0.07
Mallard duck	8.86	0.54	0.13
Mule deer	0.12	0.25	0.17
Range cattle	0.19	0.53	0.36
Spotted sandpiper	1.99	0.49	0.11

5. Conclusions

The large quantity of water that will be held in pit lakes over the next 20 years will receive increasing societal pressure to maximize their beneficial use. Hence, it is important to understand pit lake chemogenesis and any potential ecological risks in evaluating post-mining effects on the environment and pit lake use. It is also apparent, despite some uncertainty in the specifics of the predictions, that over the last decade the concerted efforts of academic, consulting and mining groups have led to a convergence of agreement on the types of water quality that may be anticipated in any given geological setting (Miller et al., 1996; Davis and Eary, 1997; Eary, 1999; Shevenell et al., 1999). At this juncture, predicting water quantity and quality

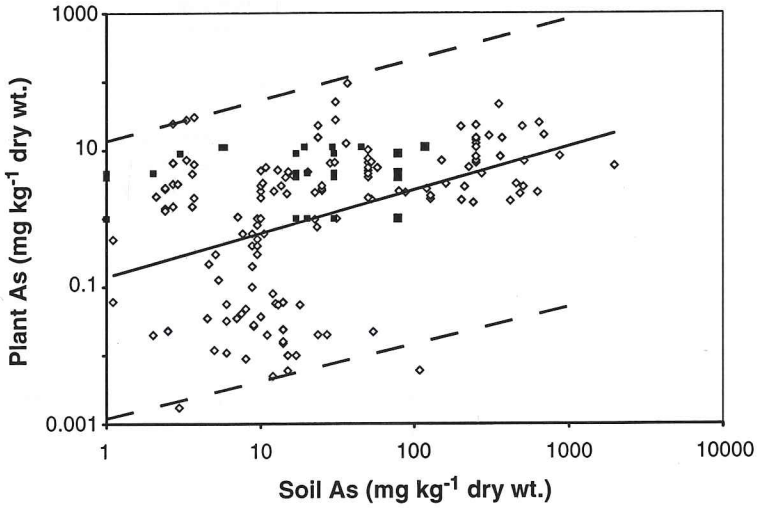

Fig. 14. Empirical As phytoconcentration data (■) compared to the ORNL (1998) data set (◊). The error bars (––) are ±2 S.D.

trends is a tractable goal, probably to within a factor of two for major ions and a factor of five for trace constituents.

Conversely, understanding ecological risks is in its infancy. However, the collection of site-specific data with which to assess bio-uptake factors, such as reported here, represents an important step in risk quantitation. This study also suggests that further investigation pertaining to prey bioavailability, as well as increased understanding of aquatic-to-terrestrial exposure in a pit lake environment is warranted to more accurately assess site ecological risk.

From a regulatory perspective, it is necessary to provide accurate predictions because the results of environmental assessments are usually compared to numerical standards. While uncertainty in model output is an integral part of the analysis, the objective is to determine the most likely outcome by understanding and accounting for variability in both the environmental assessment and the decision-making process rather than entering into an interminable epistemological debate. Finally, knowledge of the dose–response relationship between pit lake chemistry and biota could be used to help determine the need for, and nature of, any pro-active management decision that could be made during the life-of-mining to mitigate future pit lake water quality.

Acknowledgements

The authors appreciate reviews by M. Kalin and two anonymous individuals, which helped to improve the clarity and quality of this paper. We would also like to acknowledge the comments of Mike Ley (NDEP), Tom Olsen (BLM), John Gephardt (NDOW) and Glenn Miller (UNR) throughout the duration of this project. **[DR]**

References

Allison, J.D., Brown, D.S., Novo-Gradac, K.J., 1990. MINTEQA2/PRODEFA2—a geochemical assessment model for environmental systems—version 3.0 user's manual: Environmental Research Laboratory, Office of Research and Development. U.S. Environmental Protection Agency, Athens, Georgia. 106 pp.

Aposhian, H.V., 1997. Enzymatic methylation of arsenic species and other new approaches to arsenic toxicity. Annu. Rev. Pharmacol. Toxicol. 37, 397–419.

Anderson, M.P., Woessner, W.W., 1992. Applied Groundwater Modeling: Simulation of Flow and Advective Transport. Academic Press, Inc., New York. 381 pp.

ASTM, 1996. Standards on Analysis of Hydrologic Parameters and Groundwater Modeling. American Society of Testing and Materials. West Conshohocken, Penn.

Berger, D.L., 2000. Water budgets for Pine Valley, Carico Lake Valley, and Upper Reese River Valley hydrographic areas, Middle Humboldt River Basin, North-Central Nevada—methods for estimation and results. U.S. Geological Survey Water-Resources Investigation Report 99-4272.

Bitterroot, 1999. Report to Getchell Gold Corporation: Monitoring of Vegetation Reference Sites. Bitterroot Associates, Corvallis, MT.

Chapman, P.M., Fairbrother, A., Brown, D., 1998. A critical evaluation of safety (uncertainty) factors for ecological risk assessment. Environ. Toxicol. Chem. 17 (1), 99–108.

Chigbo, F.E., Wayne, R., Shore, F.L., 1982. Uptake of arsenic, cadmium, lead and mercury from polluted waters by the water hyacinth *Eichornia crassipes*. Environ. Pollut. 27, 31–36.

Cole, J.J., Caraco, N.F., Kling, G.W., Kratz, T.K., 1994. Carbon dioxide supersaturation in the surface waters of lakes. Science 265, 1568–1570.

Cole, T.M., Wells, S.A., 2002. CE-QUAL-W2: a two-dimensional, laterally averaged, hydrodynamic and water quality model, Version 3.1 (User Manual). Prepared for U.S. Army Corps of Engineers, Washington, DC.

Davis, A., 2003. A screening-level laboratory method to estimate pit lake chemistry. Mine Water Environ. 194–205.

Davis, A., Ashenburg, D., 1989. The aqueous geochemistry of the Berkeley Pit, Butte, Montana. Appl. Geochem. 4, 123–136.

Davis, A., Eary, L.E., 1997. Pit lake water quality in the western U.S.: an analysis of chemogenetic trends. Min. Eng. 98–102.

Davis, J.A., Leckie, J.O., 1978. Surface ionization and complexation at the oxide/water interface: II. Surface properties of amorphous iron oxyhydroxide and adsorption of metal ions. J. Coll. Sci. 63, 480–499.

Davis, G., Ritchie, A., 1986. A model of oxidation in pyritic mine wastes: Part 1. Equations and approximate solution. Appl. Math. Model. 10, 314–322.

Davis, A., Ruby, M.V., Bergstrom, P.D., 1992. Bioavailability of arsenic and lead in soils from the Butte, Montana Mining District. Environ. Sci. Technol. 3, 461–468.

Davis, A., Ruby, M.V., Bloom, M., Schoof, R., Freeman, G., Bergstrom, P.D., 1996. Mineralogic constraints on the bioavailability of arsenic in smelter-impacted soils. Environ. Sci. Technol. 30, 392–399.

Davis, A., Moomaw, C., Fennemore, G.G., Buffington, R., 2001. Risk-Based Closure of Mining Facilities. Remedial Actions at Industrial Sites. CRC Press, Boca Raton.

Doherty, J., 1998. Visual PEST: Graphical Model Independent Parameter Estimation. Watermark Computing and Waterloo Hydrogeologic Inc.

Drever, J.I., 1988. The Geochemistry of Natural Waters, 2nd edition. Prentice-Hall, Englewood Cliffs, New Jersey.

Dzombak, D.A., Morel, F.M.M., 1990. Surface Complexation Modeling: Hydrous Ferric Oxide. John Wiley and Sons, New York.

Eary, L.E., 1999. Geochemical and equilibrium trends in mine pit lakes. Appl. Geochem. 14, 963–987.

Eckberg, C., 2002. Uncertainties connected with geochemical modeling of waste disposal in mines. Mine Water. Environ. 21, 41–51.

Fennemore, G.G., Neller, W.C., Davis, A., 1999. Modeling pyrite oxidation in arid environments. Environ. Sci. Technol. 32, 2680–2687.

Ford, K., 1996. Risk Management Criteria for Metals at BLM Mining Sites. BLM/RS/ST-97/001+1703. Technical Note 390 (revised). Bureau of Land Management, Denver, CO.

Foster, A.L., Brown Jr., G.E., Tingle, T.N., Parks, G.A., 1998. Quantitative arsenic speciation in mine tailings using X-ray absorption spectroscopy. Am. Mineral 83, 553–568.

Garrels, R.M., MacKenzie, F.T., 1967. Origin of the chemical compositions of some springs and lakes, Equilibrium Concepts in Natural Water Systems. Am. Chem. Soc. Adv. Chem. Ser. 67, 222–242.

Geomega, 2003a. Groundwater Flow Modeling Report for the Getchell Main and North Pits. Geomega, Boulder, CO.

Geomega, 2003b. Evaluation of Expected Pit Lake Conditions, Main and North Pits, Getchell Mine. Geomega, Boulder, CO.

Geomega, 2003c. Ecological Risk Assessment for the Getchell Mine Main Pit. Geomega, Boulder, CO.

Goodyear, K.L., McNeill, S., 1999. Bioaccumulation of heavy metals by aquatic macro-invertebrates of different feeding guilds: a review. Sci. Total Environ. 229, 1–19.

Groff, J.A., Heizler, M.T., McIntosh, W.C., Norman, D.I., 1997. $^{40}Ar/^{39}Ar$ dating and mineral paragenesis for Carlin-type gold deposits along the Getchell trend: evidence for Cretaceous and Tertiary gold mineralization. Econ. Geol. 92, 601–622.

Grimes, D.J., Ficklin, W.H., Meier, A.L., McHugh, J.B., 1995. Anomalous gold, antimony, arsenic, and tungsten in ground water and alluvium around disseminated gold deposits along the Getchell Trend, Humboldt County, Nevada. J. Geochem. Explor. 52, 351–371.

Hobbs, S.W., 1948. Geology of the northern part of the Osgood Mountains, Humboldt County, Nevada. Yale University, PhD thesis.

HydroGeoLogic, 1996. MODFLOW-SURFACT, Code Documentation Report. HydroGeoLogic Inc., Herndon, VA.

James, F., Lazar, V.A., Binns, W., 1966. Effects of sublethal doses of certain minerals on pregnant ewes and fetal development. Am. J. Vet. Res. 27, 132–135.

Kalin, M., Smith, M.P., Cao, Y., 2000. Sedimentation in a pit lake in relation to water quality changes. In: Ozberk, E., Oliver, A.J. (Eds.), Proc. Int. Symp. on the Process Metallurgy of Uranium, Sept. 9–15 2000, Saskatoon, Saskatchewan, Canada.

Kalin, M., Cao, Y., Smith, M.P., Olaveson, M.M., 2001. Development of the phytoplankton community in a pit-lake in relation to water quality changes. Water Res. 35, 3215–3225.

Langdon, C.J., 2001. Survival and behaviour of the earthworms *Lumbricus rubellus* and *Dendrodrilus rubidus* from arsenate-contaminated and non-contaminated sites. Soil Biol. Biochem. 33, 1239–1244.

Langmuir, D., 1997. Aqueous Environmental Geochemistry. Prentice Hall, Upper Saddle River, NJ.

Langmuir, D., Whittemore, D.O., 1971. Variations in the Stability of Precipitated Ferric Oxyhydroxides: Non-natural Water Chemistry. Am. Chem. Soc. Symp. Ser., vol. 106, pp. 209–234. American Chemical Society, Washington, D.C.

Larocque, M., Banton, O., Ackerer, P., Razack, M., 1999. Determining Karst transmissivities with inverse modeling and an equivalent porous media. Groundwater 37, 897–903.

Lengke, M., 2001. Arsenic sulfide oxidation kinetics, PhD Dissertation. University of Nevada, Reno, NV.

McDonald, M.G., Harbaugh, A.W., 1988. A modular three-dimensional finite-difference ground-water flow model: U.S. Geological Survey Techniques of Water-Resources Investigations, Book 6.

McManus, J., Collier, R., Dymond, J., Wheat, C.G., Larson, G.L., 1996. Spatial and temporal distribution of dissolved oxygen in Crater Lake, Oregon. Limnol. Oceanogr. 41 (4), 722–731.

Meinrath, G., Merkel, B., Ödegaard-Jensen, A., Ekberg, 2004. Sorption of iron on surfaces: modeling, data evaluation, and measurement uncertainty. Acta Hydrochim. Hydrobiol. 32, 154–160.

Miller, G.C., Lyons, W.B., Davis, A., 1996. Understanding the water quality of mining pit lakes. Environ. Sci. Technol. 30, 118A–123A.

Minteau, P., Collins, B.T., Baril, A., 1996. On the use of scaling factors to improve interspecies extrapolation of acute toxicity to birds. Regul. Toxicol. Pharmacol. 24, 24–29.

Nordstrom, D.K., Archer, D.G., 2003. Arsenic thermodynamic data and environmental geochemistry. In: Welch, A.H., Stollenwork, K.G. (Eds.), Arsenic in Ground Water. Kluwer Academic.

Ödegaard-Jensen, A., Ekberg, C., Meinrath, G., 2004. LJUNGSKILE: a program for assessing uncertainties in speciation calculations. Talanta 63, 907–916.

ORNL, 1998. Empirical models for the uptake of inorganic chemicals from soil by plants. Oak Ridge National Laboratory, Oak Ridge, TN. BJC/OR-133. September.

Parkhurst, D.L., 1995. User's guide to PHREEQC—a computer program for speciation, reaction-path, advective transport, and inverse geochemical calculations. U.S. Geological Survey Water Resources Investigation Report, 95-4227.

Parshley, J.V., Bowell, R.J., 2003. The limnology of Summer Camp pit lake: a case study. Mine Water Environ. 22, 170–186.

PTI, 1992. Chemogenesis of the Gold Quarry Pit Lake, Eureka County, Nevada. Prepared for Newmont Gold Company, Denver, CO.

PTI, 1996. Chemical Composition, Limnology, and Ecology of Three Existing Nevada Mine Pit Lakes. Interim Report. April.

Rainbow, P.S., Dallinger, R., 1991. Metal uptake, regulation and excretion in freshwater invertebrates. In: Dallinger, R., Rainbow, P.S. (Eds.), Ecotoxicology of Metals in Invertebrates. Lewis Publishers, Boca Raton, FL, p. 119.

Rainbow, P.S., 2002. Trace metal concentrations in aquatic invertebrates: why and so what? Environ. Pollut. 120, 497–507.

Rodriguez, R.R., Basta, N.T., 1999. An in vitro gastrointestinal method to estimate bioavailable arsenic in contaminated soils and solid media. Environ. Sci. Technol. 33, 642–649.

Roswell, A.J., Rees, M.N., Suzcek, C.A., 1979. Margin of the North American continent in Nevada during late Cambrian time. Am. J. Sci. 279, 14–33.

Sample, B.E., Beauchamp, J.J., Suter, R.A., Suter II, G.W., 1998. Development and Validation of Bioaccumulation Models for Small Mammals. ES/ER/TM-219. February.

Savage, K.S., Ashley, R.A., Bird, D.K., 2000. Wall rock geochemical contributions to a high-arsenic, alkaline pit lake at the Jamestown Mine, California. Eos, Trans.—Am. Geophys. Union 81 (48), F525.

Schroeder, H.A., Mitchner, M., 1971. Toxic effects of trace elements on the reproduction of mice and rats. Arch. Environ. Health 23, 102–106.

Schwertmann, U., Taylor, R.M., 1977. Iron oxides. Minerals in Soil Environments. Soil Sci. Soc. Am.

Shacklette, H.T., Boerngen, J.G., 1984. Element concentrations in soils and other surficial materials on the conterminous United States. Prof. Pap.—Geol. Surv. (U.S.) 1270.

Shevenell, L., 1996. Statewide potential evapotranspiration maps for Nevada. Nevada Bureau of Mines and Geology Report, vol. 48, p. 29.

Shevenell, L., Connors, K.A., Henry, C.D., 1999. Controls on pit lake water quality at sixteen open-pit mines in Nevada. Appl. Geochem. 14, 669–687.

Sobek, A.A., Schuller, W.A., Freeman, J.R., Smith, R.M., 1978. Field and Laboratory Methods Applicable to Overburdens and Minesoils. EPA-600/2-78-054.

Spitz, K., Moreno, J., 1996. A practical guide to groundwater and solute transport modeling. Wiley, New York, NY, p. 461.

Stanley Jr., T.R., Spann, J.W., Smith, G.J., Rosscoe, R., 1994. Main and interactive effects of arsenic and selenium on mallard reproduction and duckling growth and survival. Arch. Environ. Contam. Toxico. 26, 444–451.

Tempel, R.N., Shevenell, L.A., Lechler, P., Price, J., 2000. Geochemical modeling approach to predicting arsenic concentrations in a mine pit lake. Appl. Geochem. 15, 475–492.

Thompson, S.E., Burton, C.A., Quinn, D.J., Ng, Y.C., 1972. Concentration Factors of Chemical Elements in Edible Aquatic Organisms. University of Califonia, Lawrence Livermore Laboratory, Biomedical Division, Livermore, CA. UCPL-50564.

U.S. EPA, 1985. Ambient Water Quality Criteria for Arsenic-1984. Environmental Protection Agency, Regulations and Standards Criteria and Standards Division, Washington DC. January.

U.S. EPA, 1992. Quality Assurance and Quality Control in the development and application of groundwater models, EPA/600/R-93/011. Washington D.C.

U.S. EPA, 1993a. Methods for the Determination of Inorganic Substances in Environmental Samples. 600/R-93-100. U.S. Environmental Protection Agency, Washington, D.C.

U.S. EPA, 1993. Wildlife exposure factors handbook. Volumes 1 and 2. EPA/600/R-93/187a and b. U.S. Environmental Protection Agency, Office of Research and Development, Washington D.C.

Vahter, M., Marafante, E., 1983. Intracellular interaction and metabolic fate of arsenite and arsenate in mice and rabbits. Chem. Biol. Interact. 47, 29–44.

Wetzel, R.G., 1983. Limnology. Second Edition. Saunders College Publishing, Harcourt Brace Jovanovich College Publishers, New York, NY.